

# Optimization of VVER-1200 Reactor Core Design: Enhancing Power Homogeneity and Safety

Afroza Shelley<sup>1\*</sup>, Md. Abidur Rahman Ishraq<sup>2</sup>

<sup>1</sup>Department of Nuclear Engineering, University of Dhaka, Bangladesh

<sup>2</sup>National Research Nuclear University MEPhI, Moscow, Russia

---

Mailing:

**Dr. Afroza Shelley**

Professor

Department of Nuclear Engineering,

Faculty of Engineering, University of Dhaka,

Nilkhet Road, Dhaka-1000

Bangladesh

\*E-mail: [shelley@du.ac.bd](mailto:shelley@du.ac.bd)

Phone: +880-1716012070

---

Total number of Pages: 21

Total number of Tables: 03

Total number of Figures: 07

# Optimization of VVER-1200 Reactor Core Design: Enhancing Power Homogeneity and Safety

## Abstract

This study aimed to identify the optimal VVER-1200 reactor core model through computational burnup analysis to achieve homogeneous power distribution and improved neutronic as well as safety parameters by varying assembly orientations. Eight core models each based on differently enriched fuel assemblies with varying numbers of integrated burnable absorber rods were evaluated based on key parameters such as effective multiplication factor ( $k_{eff}$ ), radial core power distribution, peaking factor (PPF), conversion ratio, and effective delayed neutron fraction, using the burnup calculation code SERPENT-2.1.32 and the ENDF/B-VII.1 nuclear data library. Model 6 showed the best performance, maintaining a  $k_{eff}$  close to 1.0 over 360 Effective Full Power Days (EFPD), with a balanced conversion ratio and the lowest PPF. A three-batch refueling scheme with a cycle length of 360 EFPD ensured sustained power generation and operational criticality. Negative fuel temperature coefficient (FTC) and moderator temperature coefficient (MTC) values across all cycles highlight inherent safety mechanisms.

**Keywords:** Flat power; power peaking factor; delayed neutron fraction, conversion ratio, VVER-1200.

## 1. Introduction

The reactor core power distribution is a vital aspect and must be managed in uniform and homogenous manner to ensure safe operation. Uniform core power distribution depends on control rod position, fuel enrichment, fuel burnup, reflector, arrangement of fuel assemblies, etc. An irregular and non-uniform core power distribution is often referred to as power tilt. Power tilt creates the problem of uneven heat distribution, risk of fuel damage, control challenges, and xenon oscillations. However, the aforementioned power tilt can be eliminated with a combination of proper core design, arrangement of fuel assemblies, and using effective way of control mechanisms [1].

The core power distribution for VVER-1000 reactor has been analyzed for cold zero power (CZP), hot zero power, and normal operational states using thermal neutronic calculation [2]. Along with neutronic parameters, two different methods of power flattening have been studied for space gas-cooled power reactor [3]. An extensive study on temperature and power distribution in molten salt reactor (MSR) has been accomplished where the heat generation in graphite moderator has been taken into consideration [4]. Several physical studies have been carried out on the power distribution in low enriched uranium (LEU) fuel of IVG.1M reactor [5]. The power distribution in very high temperature reactor assembly has been calculated utilizing Monte Carlo MVP3 code and later it has been compared with measured power distribution [6, 7]. The calculation of power distribution and power peaking factors in 3D geometry for miniature neutron reactor has been conducted [8]. A control system to produce uniform power distribution has been proposed for CANDU reactor which is successful in countering Xe induced oscillations [9]. An analysis which uses ex-core neutron detector and neural a neural network has been conducted to monitor the 3D power distribution [10]. Relative power distribution and power peaking factor have been estimated in VVER 1000 reactor using artificial neural network [11]. Several studies have been conducted on relative pin-power distributions and power peaking factor along with other neutronic and safety parameters in VVER-1000 assembly analysis [12, 13]. A very few works on power distribution analysis in diverse orientation of VVER-1200 reactor core are available and that incites us to undertake the study extensively.

VVER-1200 reactor core has been taken as a reference reactor as it is currently under construction and will be commissioned soon in our country addressed as Rooppur Nuclear Power Plant (RNPP). Numerous approaches to improve the fuel cycle, proliferation characteristics, and burnup characteristics of the VVER-1200 reactor were investigated in a number of our earlier research papers [14-18]. Ensuring uniform and symmetry core power distribution and low power peaking factor along with other neutronic and safety parameters for the reactor core is a dire need to circumvent power tilt and anomalies associated non-uniform power distribution. Under the circumstances, we are targeting to conduct a study that will work with diverse core orientations to determine possible better core orientation for homogenous, symmetrical core power distribution with low power peaking factor. The findings of this study might be significant for reactor physicists and operators, as they provide valuable insights into core design strategies that balance higher burnup levels with reduced power peaking. By identifying core models with

lower PPF values and a flatter radial power distribution, reactor performance can be optimized while ensuring the safe and efficient operation of VVER 1200 reactors, specifically for the RNPP project.

## 2. Core description and designed core

The design parameters of the VVER-1200/AES-2006 reactor core which has been utilized in this research work are presented in Table 1.

**Table 1:** Technical parameters of the VVER-1200 core [5, 22, 23].

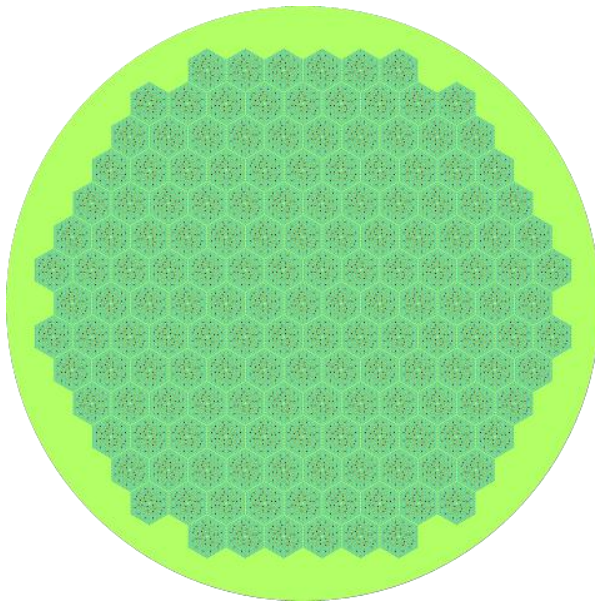
Components	Parameters	Values
Reactor Core	Rated thermal power ( $MW_{th}$ )	3200
	Rated electrical power ( $MW_e$ )	1200
	Coolant & moderator	water + boric acid
	Coolant inlet temperature ( $^{\circ}C$ )	298.2
	Coolant outlet temperature ( $^{\circ}C$ )	328.9
	Fuel rod material	UO <sub>2</sub>
	IBA rod material	UO <sub>2</sub> + 4% Gd <sub>2</sub> O <sub>3</sub>
	Number of fuel assemblies	163
	Core/fuel active section height (m)	3.75
	Core equivalent diameter (m)	3.16
	Average core power density ( $MW/m^3$ )	108.5
Fuel assembly	Shape of the assembly	Hexagonal
	Total number of rods	331
	Number of fuel rods	312
	Number of guide thimbles	18
Fuel element	Pellet hole radius (cm)	0.06
	Pellet outer radius (cm)	0.38
	Clad thickness (cm)	0.0685
	Pin pitch (cm)	1.275
	Density of fuel ( $g/cm^3$ )	10.97
	Density of Gd <sub>2</sub> O <sub>3</sub> ( $g/cm^3$ )	7.41
	Material of fuel clad/gap	E110/Helium
	Boron concentration in moderator (ppm)	600

Eight (08) different full-core models of VVER 1200 reactor have been addressed to conduct the study. The models have been introduced based on the orientation of the different enriched fuel assemblies and the number of IBA rods. The optimize IBA rods for different enriched assembly

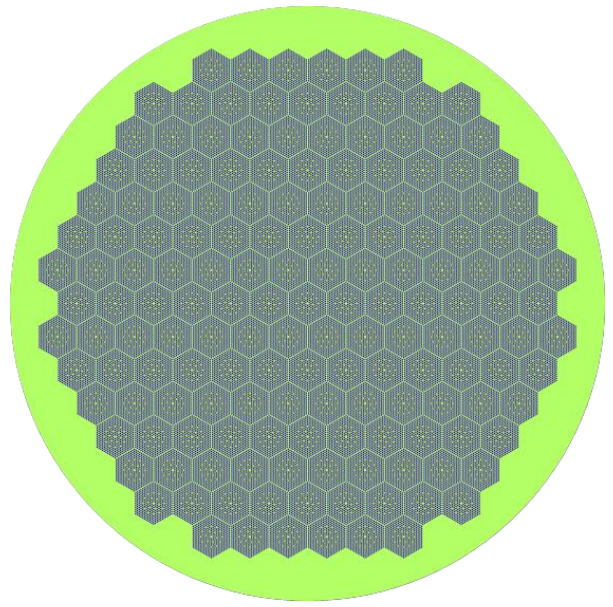
that have been used are 30, 24, 18, 18, 12, and 8 IBA rods for 4.95%, 4.5%, 4.0%, 3.5%, 3.0%, and 2.5% wt.% U-235 respectively. There are no IBA rods in 2.0% U-235 enriched assembly. The detailed description of the proposed core models has been presented in Table 1. Radial view of the designed models has been shown in [Figure 1](#). The detailed neutronic calculations have been accomplished using SERPENT 2.1.32 [\[19\]](#) and ENDF/B-VII.1 nuclear data library [\[20\]](#). SERPENT is Monte Carlo reactor physics simulation software, developed by the VTT Technical Research Centre of Finland. Meulekamp's method [\[21\]](#) has been addressed in this study to calculate the effective delayed neutron fraction.

**Table 1:** Description of the designed core models

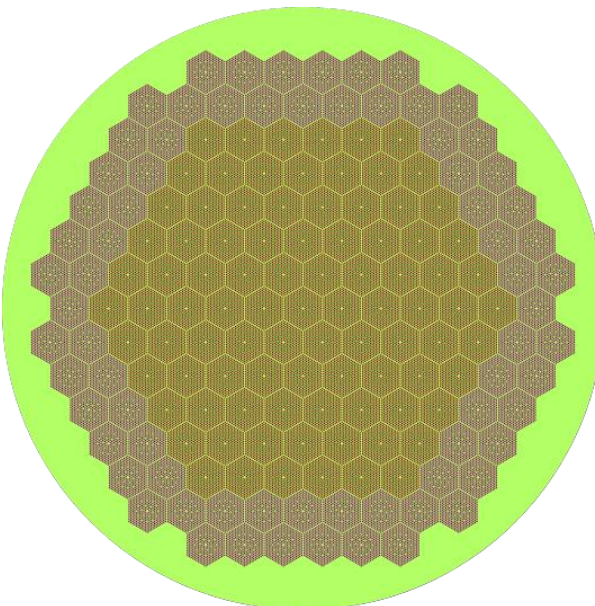
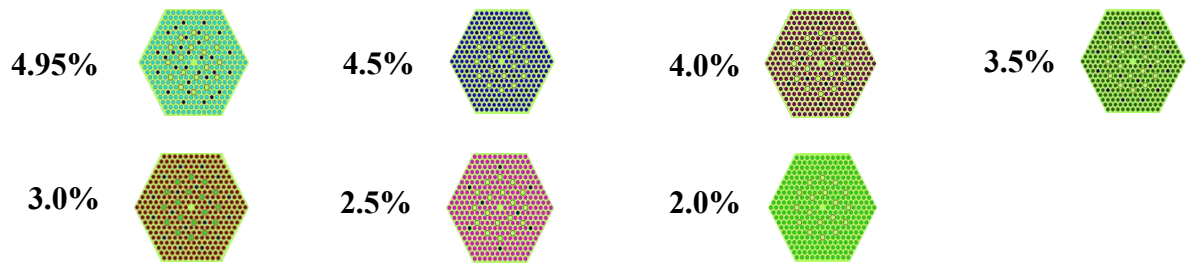
<b>Model ID</b>	<b>Number of FAs</b>	<b>Enrichment of fuel (wt.%)</b>	<b>Number of IFBA rods per assembly</b>
Model-1	163	4.95	30
Model-2	163	4.5	24
Model-3	72	3.0	12
	91	4.0	18
Model-4	72	2.5	8
	91	4.0	18
Model-5	72	3.0	12
	37	4.0	18
	54	4.5	30
Model-6	37	3.0	12
	24	3.5	18
	30	4.0	18
	36	4.5	24
	36	4.95	30
Model-7	19	2.5	8
	18	3.0	12
	24	3.5	18
	30	4.0	18
	36	4.5	24
	36	4.95	30
Model-8	7	2.0	N/A
	12	2.5	8
	18	3.0	12
	24	3.5	18
	30	4.0	18
	36	4.5	24
	36	4.95	30



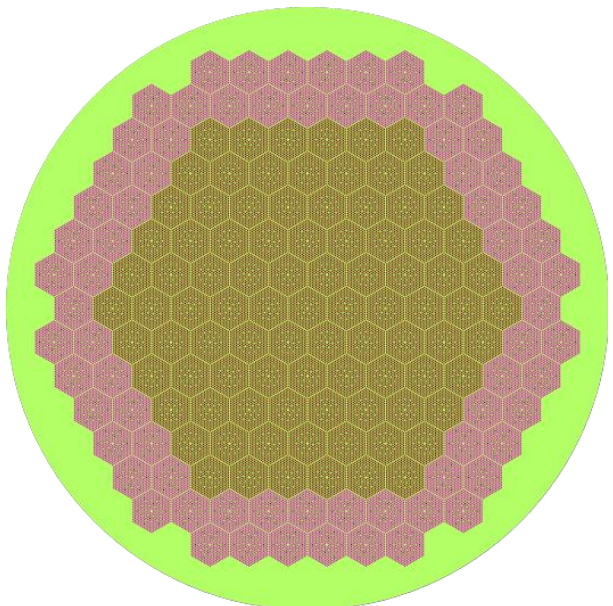
Model 1



Model 2



Model 3



Model 4

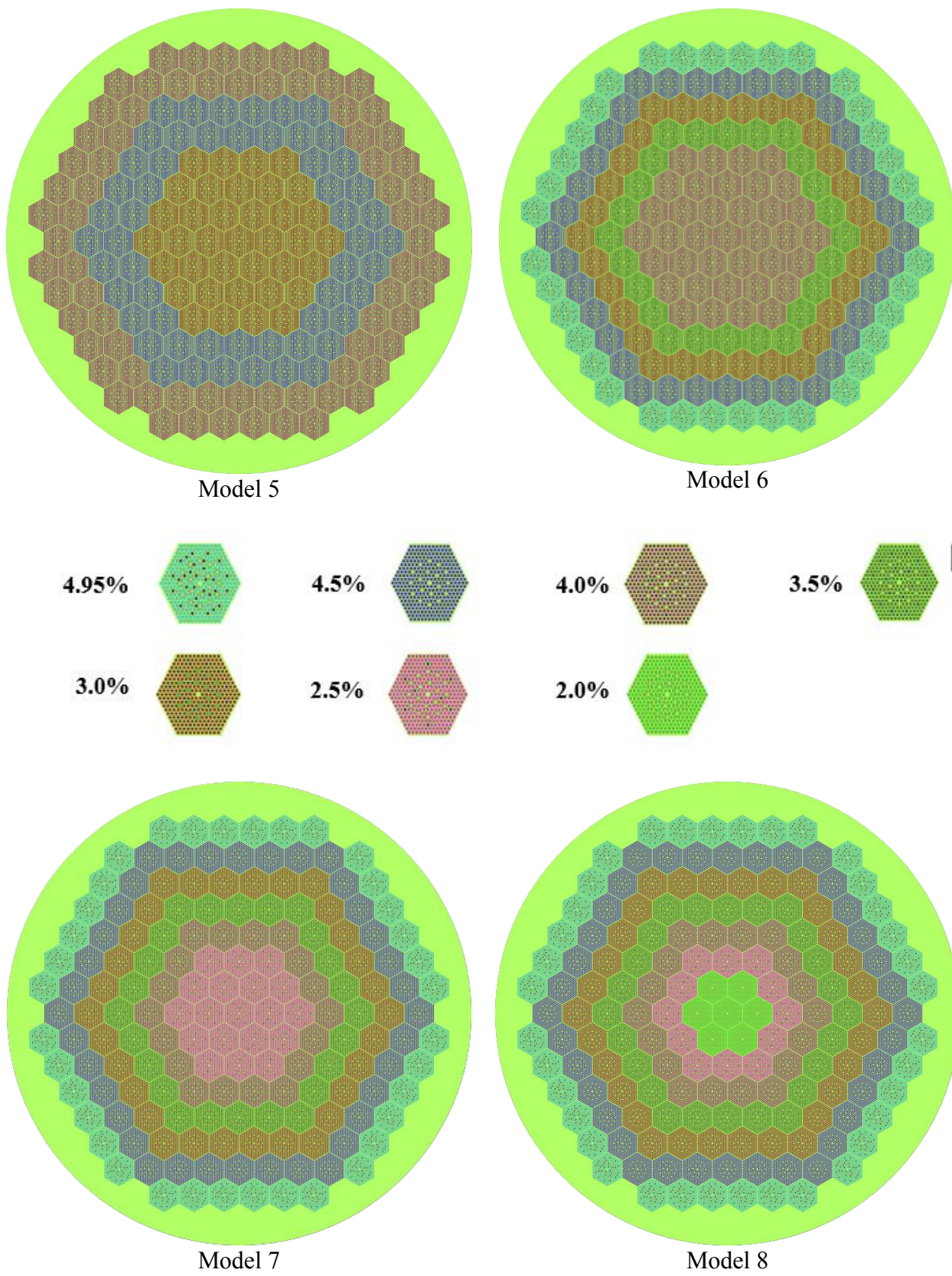


Fig. 1: The modeled cores configuration

### 3. Results & Discussion

#### 3.1. *Effective Multiplication Factor ( $k_{\text{eff}}$ )*

The effective multiplication factor ( $k_{\text{eff}}$ ) is a vital parameter in the context of predicting the nuclear reactor's behavior and stability, criticality analysis, ensuring safe and controlled operation, and optimizing fuel usage. For the first cycle of burnup, the effective multiplication factors for all models are shown in Fig. 2. As we know, the  $k_{\text{eff}}$  depends on several factors including fuel type, fuel enrichment, total loaded fissile content, the presence of IBA, type of the moderator, and the arrangement of different enriched assembly etc. In this study, all the factors are constant for different models except the arrangement of different enriched assembly, total loaded fissile content and the presence of IBA. Figure 2 shows that the impact of Integral Fuel Burnable Absorber (IFBA) rods diminishes after 20 Effective Full Power Days (EFPD) for all models and  $k_{\text{eff}}$  begins to increase as the burnable absorber effect wanes. Interestingly, Model 1, despite having the highest fissile content at the BOL, does not exhibit the highest  $k_{\text{eff}}$ . Once the burnable absorber influence diminishes, Model-1 shows a pronounced increase in  $k_{\text{eff}}$ , reaching a higher at EOC. Conversely, Model 4 exhibits the lowest EOC  $k_{\text{eff}}$  due to its minimal fissile content. It is found that, the fluctuation of  $k_{\text{eff}}$  with burnup decreases when different enriched assemblies are used in core instead of single enriched assemblies. Therefore, Model 6, 7 and 8 shows the least variation of  $k_{\text{eff}}$  from BOC to EOC, due to the orientation of different enriched assemblies.

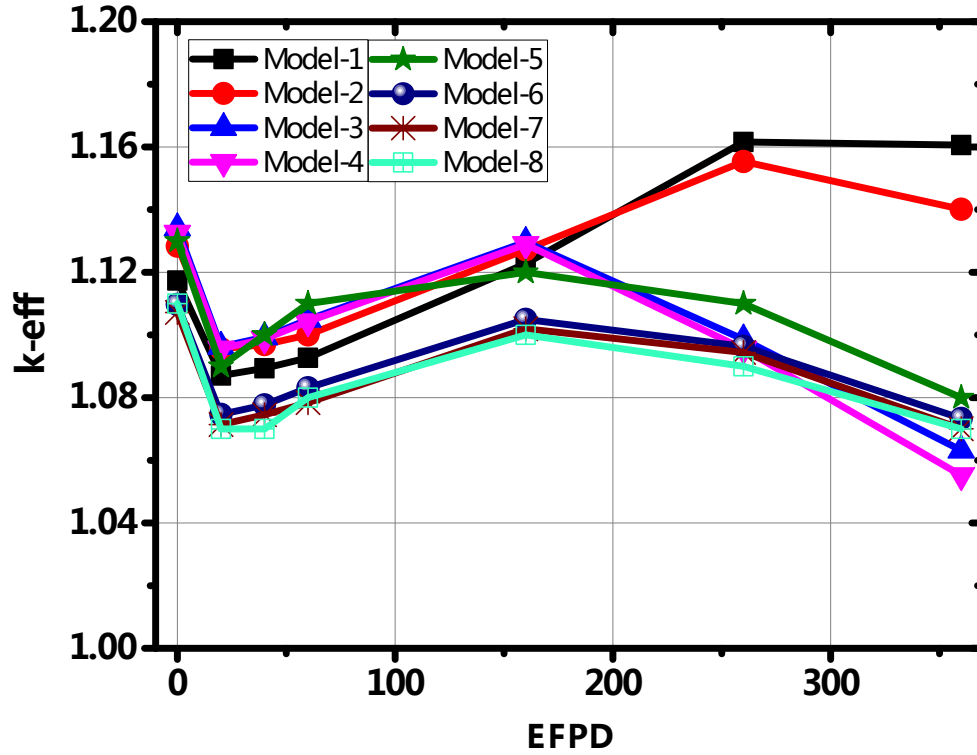


Figure 2: Variations of multiplication factor with burnup for 1<sup>st</sup> cycle

### 3.2 Radial core power distribution

The distribution of core power as a function of radial position of the assembly along the centerline of the core is shown in Fig 3. Flat core power distribution is always desirable to eliminate the problem of hot spots, the localized fuel damage, to obtain stable temperature throughout the core etc. It is found that the arrangement of different enriched fuel assembly in the core highly affects the core radial power distribution. Figure 3 shows the radial core power distribution in the central line 13 assemblies at 0 EFPD (BOL), 180 EFPD (MOC), and 360 EFPD (EOC). Model 1 and Model 2 exhibit clear spike of the core power namely hot spot at centre of the core at 0 EFPD , 180 EFPD, and 360 EFPD and the power contribution ratio of innermost assembly (hot spot) to outermost assembly (cold spot) are (4.81, 5.08), (4.92, 4.90), and (4.70, 4.65). Model 6, 7 and 8 shows comparatively flatter power distribution in the central line at BOL. However, for these models at MOC and EOC the power distribution looks uneven. In order to get the overall power profiling the value of Power Peaking Factor (PPF) must be analysed.

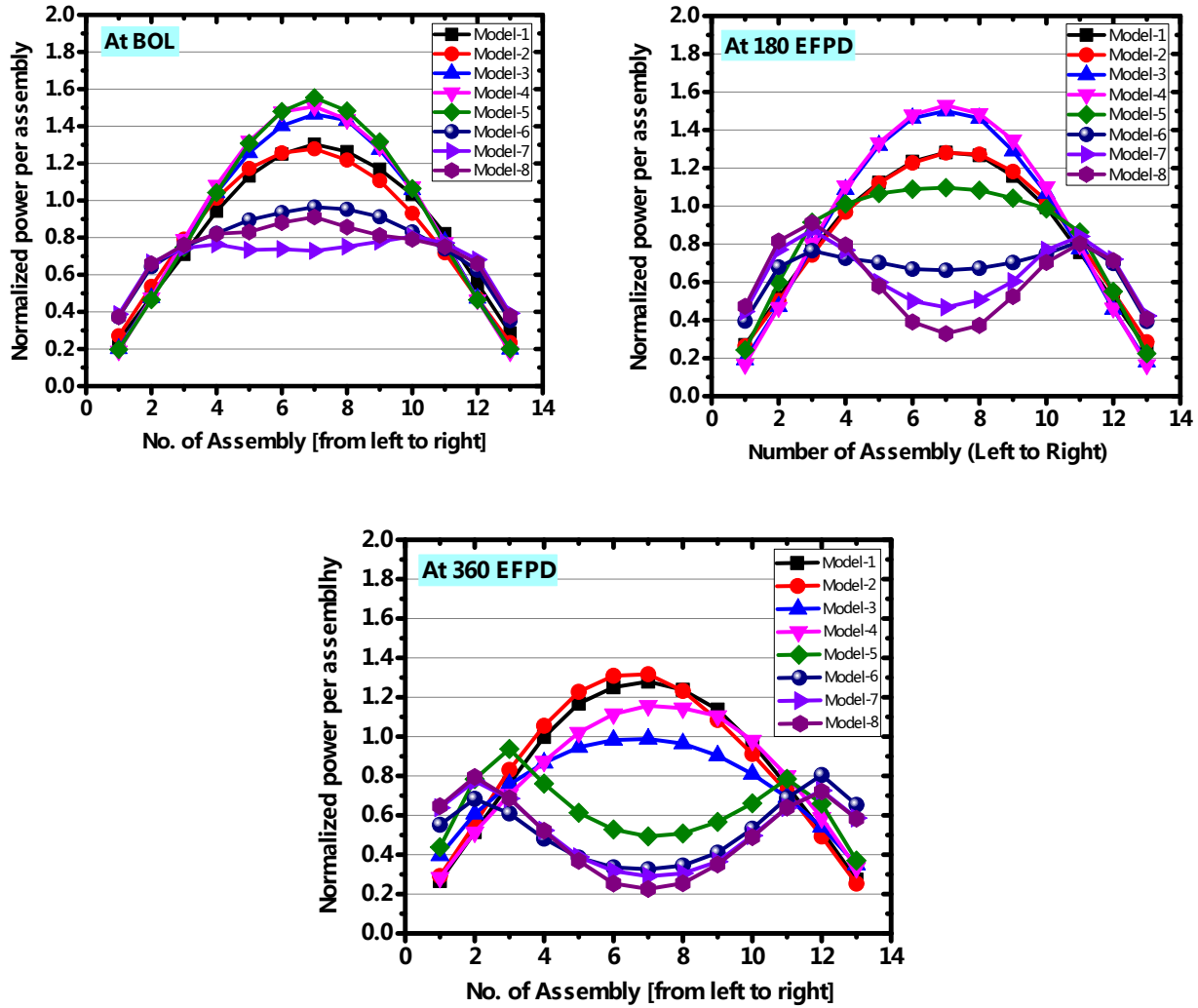


Figure 3: Radial core power distribution along the centerline [left to right] of the core.

### 3.3 Radial Power Peaking Factor (PPF)

The radial power peaking factor (PPF) is a critical parameter in nuclear reactor physics that quantifies the non-uniform distribution of power generation within the reactor core. It's calculated by dividing the maximum power of the fuel assemblies by the average power across the entire core. A high PPF signifies a concentrated zone of power generation, which can lead to fuel cladding overheating, thermal stress, and potential safety concerns. Therefore, reactor designers and operators strive to maintain an PPF within safe limits through fuel management strategies and control rod positioning. The design value of radial power peaking factor of VVER-

1200 reactor is 1.5 [6]. In the actual operation of the reactor when all the control systems are working the value of PPF must not exceed the critical value. However, in this study, no control system was applied except soluble boric acid. So, the obtained values can be more than 1.5. In Table 2, the radial PPF of all the models at 0 EFPD, 180 EFPD and 360 EFPD is presented. It can be seen that model 7 shows the least PPF value at BOL ( $1.41 < 1.5$ ) without using any control rods. With the progress of burnup the value of PPF increases for this model indicating the burnup process is decreasing the uniformity of power distribution. Only model 6 has PPF near the design value ( $1.57 > 1.5$ ) at BOL which can be control using control rods and with the progress of burnup the PPF decreases and comes under the design value. So, for further analysis Model 6 is considered as proposed model. However, some other parameters such as conversion ratio and effective delayed neutron fraction are observed in the next sections.

**Table 2:** Radial Power Peaking Factors of all the models

Model number	PPF		
	0 EFPD	180 EFPD	360 EFPD
Model 1	2.12	2.09	2.09
Model 2	2.08	2.09	2.15
Model 3	2.39	2.45	1.61
Model 4	2.46	2.49	1.89
Model 5	2.53	1.79	1.60
Model 6	1.57	1.48	1.47
Model 7	1.41	1.43	1.55
Model 8	1.49	1.61	1.48

### 3.3 Conversion Ratio

Figure 4 presents the conversion ratios for each model which reveals a trend of increasing conversion ratio with burnup for all the models. This can be attributed to the depletion of fissile isotopes (like U-235) through fission during reactor operation. As the fissile content decreases, the relative abundance of fertile isotopes (like U-238) increases within the fuel assembly. This creates a more favourable environment for neutron capture by U-238, leading to the production of fissile Pu-239 and a subsequent rise in the conversion ratio. Consequently, Model 4, with the lowest initial fissile content and highest fertile content, exhibits the highest conversion ratio amongst all the models.

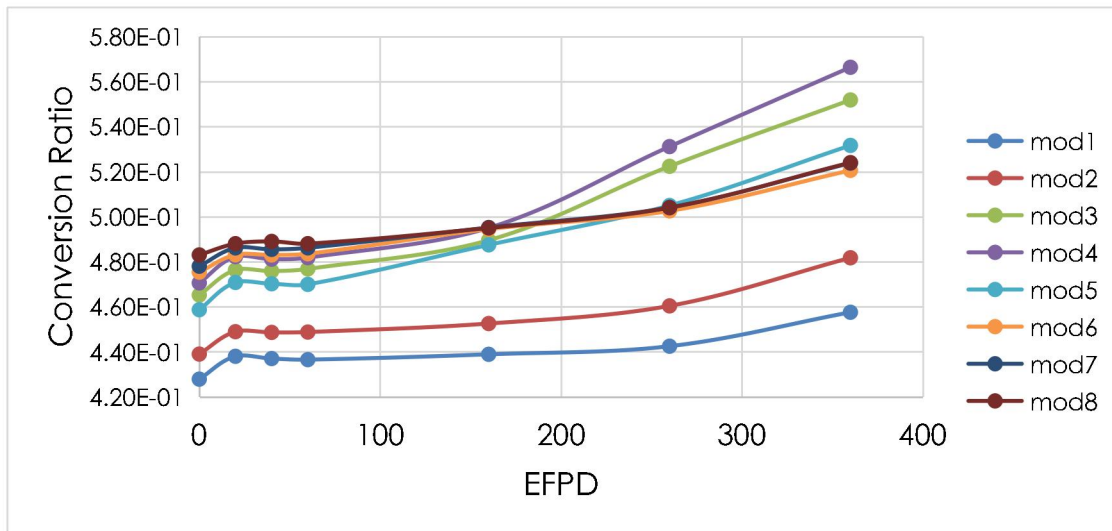
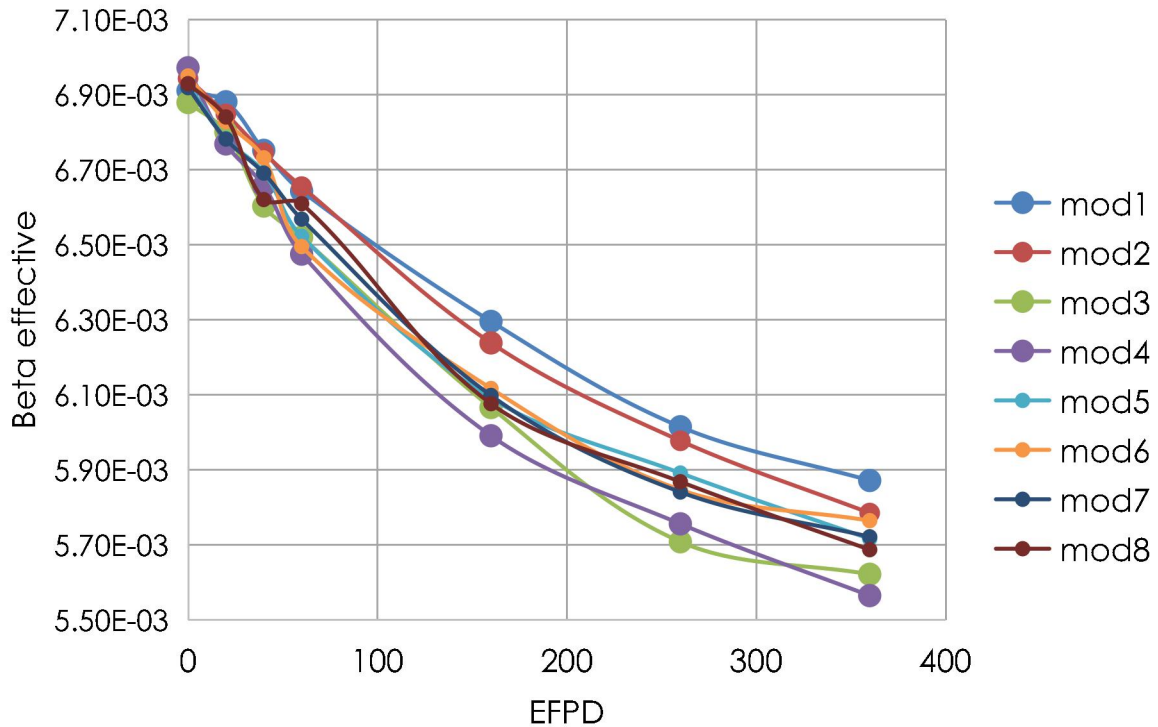


Figure 4: Changes of Conversion Ratio with burnup

### 3.4 Delayed Neutron Fraction

The effective delayed neutron fraction that influences reactor behavior and kinetics is an important parameter for reactor stability, controlled and safe operation. The effect of different model on delayed neutron fraction has been depicted in Figure 5. Meulekamp's method has been addressed in this study to calculate the effective delayed neutron fraction using SERPENT. Figure 5 exhibits that all models have shown almost same value (0.0069) of the delayed neutron fraction at BOC and it get decreased with the burnup period. For model 3, the value of the delayed neutron fraction at EOC is 64% of the BOC. The fission rate of Pu-239 and Pu-241 gets

increased with the burnup period whereas the fission rate of U-235 gets reduced [13]. It is important to note that the Pu-239 generates 0.002 delayed neutrons per fission whereas U-235 produces 0.0065 delayed neutrons per fission [1]. This discrepancy in the number of delayed neutrons generated could potentially be a contributing factor to the observed differences in delayed neutron fraction with the burnup period. As previously mentioned, the fuel conversion ratio is lower for model 1, it might experience lower fission rate of Pu-239 and Pu-241 and results in a higher value of the delayed neutron fraction at EOC.



+

Figure 5: Changes of delayed neutron fraction with burnup

After observing the results of PPF, radial power distribution, conversion ratio and effective delayed neutron fraction, model 6 is considered to be the best model. Detailed burnup calculation of this model is presented in the following sections.

### ***3.4 Three-Batch Refuelling Scheme of Model 6 for Burnup Analysis:***

Nuclear reactors require continuous criticality for sustained power generation. However, as fuel undergoes fission over time, its fissile isotope content depletes, leading to a decrease in reactivity (criticality). To maintain criticality and ensure reactor operation, a common practice is refuelling. In this analysis, a three-batch refuelling (360 EFPD cycle length) scheme is investigated for the Model-6. [Figure 6](#) illustrates the core loading pattern for this refuelling strategy. Subsequent burnup analysis results are presented in [Figure 7](#). Green colour assemblies were refuelled at 360 EFPD, blue colour assemblies were refuelled at 720 EFPD and brown assemblies are required to be refuelled at 1080 EFPD. An iterative process was employed to determine the optimal fuel reloading pattern. This procedure involved simulating various reloading scenarios and evaluating their impact on the Radial Power Peaking Factor (PPF). The primary objective was to identify a reloading pattern that minimizes PPF while ensuring the core maintains criticality throughout the operational cycle. This approach balances safety considerations (low PPF) with operational requirements (criticality for power generation).

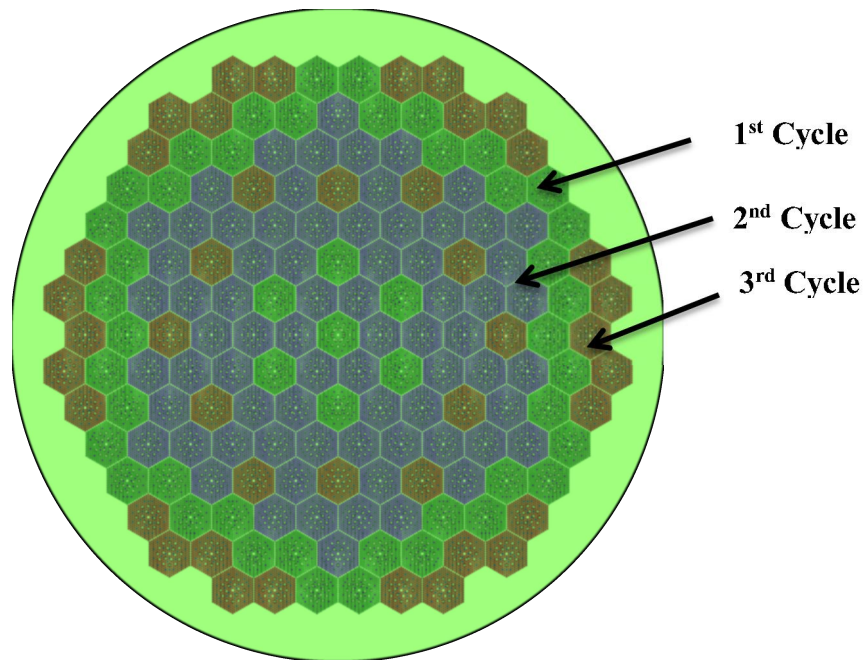


Figure 6: Core loading pattern for this refuelling strategy of Model 6

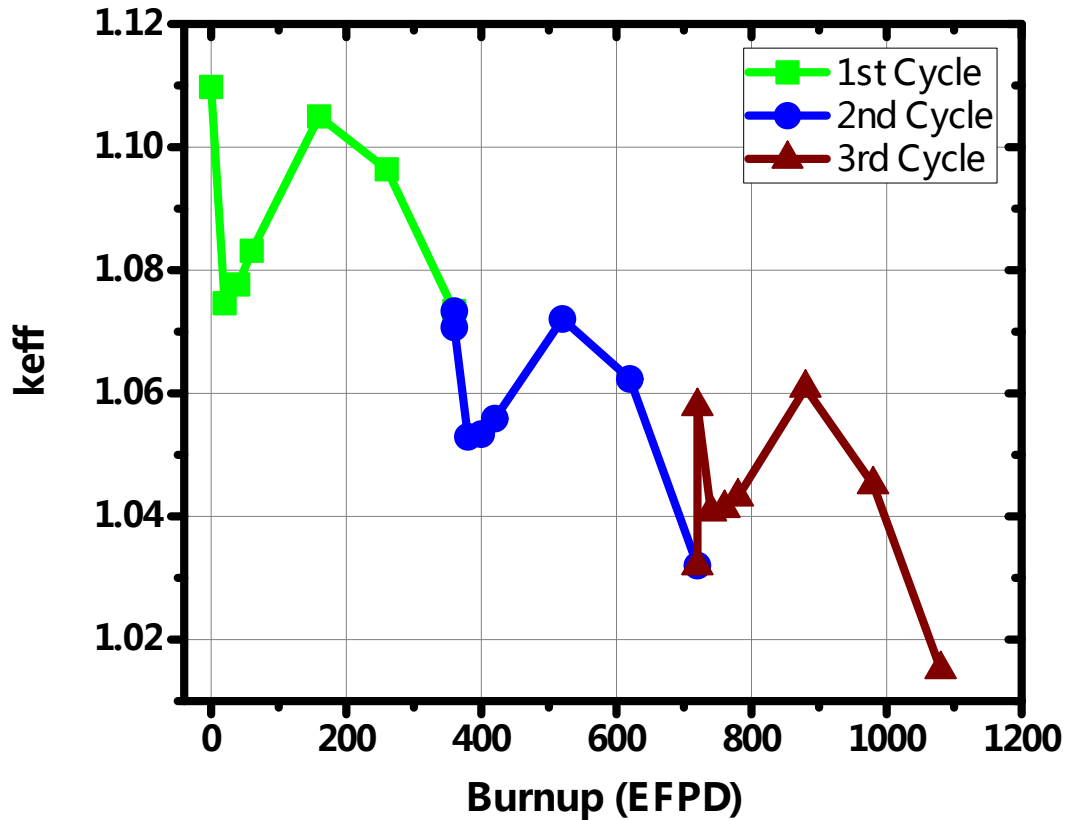


Figure 7: Variations of multiplication factor of Model 6 during the three batch refuelling scheme

Figure 7 shows a gradual reduction in  $k_{eff}$  as burnup increases across cycles, which is expected due to fuel depletion and the accumulation of fission products. In the first cycle,  $k_{eff}$  starts above 1.12, indicating higher initial reactivity at BOL to compensate for burnup and the resulting reactivity loss. As burnup progresses,  $k_{eff}$  decreases but stays above 1.0, ensuring the reactor remains supercritical and can sustain power generation. In the second cycle,  $k_{eff}$  follows a similar trend but starts at a slightly lower value due to the reduced fissile content and partially spent fuel from the previous cycle. By the third cycle,  $k_{eff}$  begins near 1.08 but continues the same downward trend, remaining close to 1.0 even at EOC, ensuring operational criticality.

### 3.5 Temperature Reactivity Coefficients

Nuclear reactors rely on delicate balances, and reactivity coefficients play a critical role in maintaining these balances. By considering these, fuel temperature coefficient (FTC) and moderator temperature coefficient (MTC) for both at BOC and EOC are measured for every fuel cycle, these coefficients assess the reactor's response to temperature changes in fuel and moderator. Table 3 shows the values of FTC and MTC at BOC and EOC of all the cycles that were observed in this study. Importantly, all observed values are negative, signifying a crucial safety feature. The values of FTC and MTC do not change very significantly as all the values are very small (in pcm) and in Monte Carlo based programs statistical error affects small values.

Table 3: FTC and MTC values at BOC and EOC of each fuel cycle of Model 6		
Observation point	FTC, pcm/K	MTC, pcm/K
BOC-1	-3.25	-11.71
EOC-1	-2.75	-28.59
BOC-2	-1.99	-38.99
EOC-2	-2.45	-35.25
BOC-3	-2.17	-35.80
EOC-3	-1.82	-30.91

## Conclusion

Different orientation of VVER-1200 reactor core has been carried out to achieve flatter power distribution as well as better neutronic and safety parameters than the conventional one. For this purpose, eight core models were investigated, by focusing on key performance parameters that influence reactor safety, stability, and fuel efficiency.

The analysis of  $k_{\text{eff}}$  revealed that Models 5, 6, and 8 maintained  $k_{\text{eff}}$  values closest to 1.0 throughout the simulated burnup period (360 Effective Full Power Days, EFPD), indicating their ability to sustain criticality for power generation. In terms of radial power distribution, Model 6 exhibited a significant advantage. At BOL, it achieved the flattest profile among all models, with a power peaking factor (PPF) of 1.57, which is very close to the design safety limit of 1.5. While all models exhibited some degree of power peaking with burnup, Model 6 maintained the lowest PPF compared to others, reaching 1.47 at EOC. Model 4, with the lowest initial fissile content and highest fertile content, achieved the highest conversion ratio, reaching 0.72 at EOC. However, Model 6 also demonstrated a respectable conversion ratio, reaching 0.68 at EOC with a more balanced fissile and fertile content. All models converged towards a similar delayed neutron fraction at EOC (around 0.004), Model 1 displayed the highest value (0.0052) due to its higher initial fissile content and consequently, a larger contribution from U-235 fission. Furthermore, a three-batch refuelling scheme with a cycle length of 360 EFPD was studied for Model 6 and found that  $k_{\text{eff}}$  remains above 1.0, throughout all three cycles, highlighting the reactor's ability to stay supercritical and operationally critical even as burnup progresses. This behavior indicates that the reactor Model 6 is effectively designed for stable, long-term operation with efficient fuel utilization across multiple cycles. Finally, the fuel temperature coefficient (FTC) and moderator temperature coefficient (MTC) were determined for each fuel cycle of models 6. All observed values were negative, ranging from -1.82 pcm/K to -3.25 pcm/K for FTC and -11.71 pcm/K to -38.99 pcm/K for MTC. These negative coefficients indicate inherent self-regulating safety mechanisms within the reactor design, as a temperature increase leads to a decrease in reactivity, helping to maintain criticality control.

The authors acknowledge the financial support for this study is the Bangladesh Bureau of Educational Information and Statistics (BANBEIS). Project ID: ET 2022-2205

## References

1. “DOE FUNDAMENTALS HANDBOOK Nuclear Physics and Reactor Theory”, 1993. Volume 2 of 2, U.S Department of Energy, Washington, DOE-HDBK-1019/2-93.
2. Karahroudi, M.R., and Shirazi, S.A.M., 2015. “Study of power distribution in the CZP, HFP and normal operation states of VVER-1000 (Bushehr) nuclear reactor core by coupling nuclear codes”, *Annals of Nuclear Energy*, Volume 75, Pages 38-43, <https://doi.org/10.1016/j.anucene.2014.07.038>
3. He, Y., Cheng, K., Qiu, Z., You, E., Yang, W., Tan, S., and Zhao, F., 2021. “Research on power flattening method and neutron characteristic analysis of a megawatt-class space gas-cooled fast reactor”, *Annals of Nuclear Energy*, Volume 161, 108456, <https://doi.org/10.1016/j.anucene.2021.108456>
4. Hanusek, T., and Juan, R.M., 2021. “Analysis of the Power and Temperature distribution in molten salt reactors with TRACE. Application to the MSRE”, *Annals of Nuclear Energy*, Volume 157, 108208, <https://doi.org/10.1016/j.anucene.2021.108208>
5. Sabitova, R.R., Popov, Y.A., Irkimbekov, R.A., Bedenko, S.V., Prozorova, I.V., Svetachev, S.N., and Medetbekov, B.S., 2023. “Experimental studies of power distribution in LEU-fuel of the IVG.1M reactor”, *Applied Radiation and Isotopes*, Volume 200, 110942, <https://doi.org/10.1016/j.apradiso.2023.110942>
6. Ovi, M.H., Shelley, A., Prodhan, MH. (2021). “Neutronic analysis of VVER-1000 MOX fuel assembly with burnable absorber Gadolinia and Erbia” *Annals of Nuclear Energy* 160, 108389, <https://doi.org/10.1016/j.anucene.2021.108389>
7. Simanullang, I.L., Nakagawa, N., Ho, H.Q., Nagasumi, S., Ishitsuka, E., Iigaki, K., and Fujimoto, N., 2022. “Evaluation of power distribution calculation of the very high temperature reactor critical assembly (VHTRC) with Monte Carlo MVP3 code”, *Annals of Nuclear Energy*, Volume 177, 109314, <https://doi.org/10.1016/j.anucene.2022.109314>
8. Dawahra, S., and Khattab, K., 2011. “Calculation of the power distribution in the fuel rods of the low power research reactor using the MCNP4C code”, *Annals of Nuclear*

Energy, Volume 38, Issue 12, Pages 2859-2862,  
<https://doi.org/10.1016/j.anucene.2011.07.026>

9. Xia, L., Jiang, J., and Luxat, J.C., 2014. "Power distribution control of CANDU reactors based on modal representation of reactor kinetics", Nuclear Engineering and Design, Volume 278, Pages 323-332, <https://doi.org/10.1016/j.nucengdes.2014.05.048>
10. Xia, H., Li, B., Liu, J., 2014. "Research on intelligent monitor for 3D power distribution of reactor core", Annals of Nuclear Energy, Volume 73, Pages 446-454, <https://doi.org/10.1016/j.anucene.2014.07.033>
11. Pirouzmard, A., Dehdashti, M.K., 2015. "Estimation of relative power distribution and power peaking factor in a VVER-1000 reactor core using artificial neural networks", Progress in Nuclear Energy, Volume 85, Pages 17-27, <https://doi.org/10.1016/j.pnucene.2015.06.001>
12. Ahmed, M.T., Shelley, A., Hosen, N., 2023. "Neutronic Analysis and Fuel Cycle Parameters of Transuranic-UO<sub>2</sub> Fueled Dual Cooled VVER-1000 Assembly", Journal of Nuclear Engineering and Radiation science, <http://dx.doi.org/10.1115/1.4063757>
13. Ahmed, M.T., Shelley, A., 2023. "Annular fuel for VVER-1000 reactor: Moderation impact on neutronic behaviour", Progress in Nuclear Energy, Volume 165, 104907, <https://doi.org/10.1016/j.pnucene.2023.104907>
14. S. Sabhasachi, Koushik, R., Souvik, R., Asfakur, R., and Zahid, H. (2018). "Rooppur nuclear power plant: Current status & feasibility," Strojnícky casopis – Journal of Mechanical Engineering, volume 68, pp. 167–182, <http://dx.doi.org/10.2478/scjme-2018-0033>
15. Shelley, A., and Ovi, M.H., (2021). "Use of americium as a burnable absorber for VVER-1200 reactor", Nuclear Engineering and Technology, Volume 53, Issue 8, August 2021, Pages 2454-2463, <https://doi.org/10.1016/j.net.2021.02.024>
16. Sharmin, F., Ovi, M. H., & Shelley, A. (2023). Radiotoxicity analysis of the spent nuclear fuel of VVER-1200 reactor. *Progress in Nuclear Energy*, 156, 104538.
17. Shelley, A., & Ovi, M. H. (2022). Possibility of curium as a fuel for VVER-1200 reactor. *Nuclear Engineering and Technology*, 54(1), 11-18.

18. Shelley, A., Sharmin, F., Dipa, B., Ovi, M. H., & Salahuddin, M. (2022). Three-stage fuel option for VVER-1200 reactor. *Annals of Nuclear Energy*, 171, 109025. 2454-2463, <https://doi.org/10.1016/j.net.2021.02.024>
19. Leppänen, J., et al. (2015). “The Serpent Monte Carlo code: Status, development and applications in 2013.” *Annals of Nuclear Energy*, 82. pp. 142-150. <https://doi.org/10.1016/j.anucene.2014.08.024>
20. Smith, L.D. (2011). “Evaluated Nuclear Data Covariances: The Journey From ENDF/B-VII.0 to ENDF/B-VII.1,” *Nuclear Data Sheets*, vol. 112, pp. 3037-3053, <https://doi.org/10.1016/j.nds.2011.11.004>
21. Meulenlamp, E.A. (1998). “Synthesis and growth of ZnO nanoparticles,” *The Journal of Physical Chemistry B*, vol. 102, pp. 5566–5572.